Acta Crystallographica Section B
Structural Science
ISSN 0108-7681

Structural characterization of crystals of α-glycine during anomalous electrical behaviour

Paul Langan,[a]* Sax A. Mason,[b] Dean Myles[c] and Benno P. Schoenborn[a]

[a]Biosciences Division, Los Alamos National Laboratory, Los Alamos, NM 87545, USA, [b]Institut Laue Langevin, Avenue des Martyrs, BP 156, 38042 Grenoble CEDEX 9, France, and [c]European Molecular Biology Laboratory Outstation, Avenue des Martyrs, 38042 Grenoble, France

Correspondence e-mail: langan_paul@lanl.gov

Received 4 December 2001
Accepted 5 March 2002

The crystal structure of α-glycine has been investigated in the temperature range 288–427 K using neutron diffraction. The molecular structure does not change significantly and the putative crystallographic phase transition associated with anomalous electrical behaviour in this temperature range is not observed. The unit cell expands anisotropically with increasing temperature, with the unique monoclinic *b* axis, corresponding to the stacking direction of molecular layers, changing the most. The increasing separation of antiferroelectric molecular layers with increasing temperature is driven by an increase in molecular libration about an axis that lies perpendicular to the *b* axis. There is also a weakening of the interlayer hydrogen bonds with temperature. These structural and dynamic changes will affect the response of molecular dipoles to an applied electric field and provide a possible mechanism for the anomalous electrical behaviour.

1. Introduction

Glycine, the smallest among the amino acids, functions as a neurotransmitter and is one of the principle components of structural proteins, enzymes and hormones. The functional groups exhibit complex chemical behaviour; glycine crystallizes into three polymorphic zwitterions, α, β and γ, but converts to its nonionic form upon vaporization. Glycine can adopt a cationic, zwitterionic, or anionic form depending on pH. Depending on temperature, glycine is adsorbed onto metal substrates in deprotonated or nonionic forms (Nyberg *et al.*, 2000).

The crystal structures of α-glycine (Albrecht & Corey, 1939), β-glycine (Iitaka, 1960) and γ-glycine (Iitaka, 1961) were determined first by X-ray diffraction. Crystals of β-glycine are metastable and transform into the α or the γ form. Crystals of γ-glycine transform into the α form when heated to 438 K. Neutron diffraction studies have subsequently provided accurate position and displacement parameters for hydrogen atoms in crystals of α-glycine at around room temperature, ∼298 K (Jonsson & Kvick, 1972; Power *et al.*, 1976) and γ-glycine at 83 and 298 K (Kvick *et al.*, 1980). Electron density studies of the effects of hydrogen bonding in α-glycine have been carried out at 120 and 298 K using X–N difference Fourier methods (Almof *et al.*, 1973; Legros & Kvick, 1980). All three crystal forms of glycine have also been studied by solid-state theoretical modelling methods (Peeters *et al.*, 1975).

The polymorphs have similar internal molecular structures but differ in the way molecules are packed (the space groups are $P2_1/n$, $P2_1$ and $P3_2$, for the α, β and γ forms, respectively). The crystal structure of the most stable form, α-glycine,

Table 1
Experimental details.

	288 K	301 K	304 K
Crystal data			
Chemical formula	$C_8H_{20}N_4O_8$	$C_8H_{20}N_4O_8$	$C_8H_{20}N_4O_8$
Chemical formula weight	300.24	300.24	300.24
Cell setting, space group	Monoclinic, $P2_1/n$	Monoclinic, $P2_1/n$	Monoclinic, $P2_1/n$
a, b, c (Å)	5.0993 (3), 11.9416 (6), 5.4608 (3)	5.0999 (3), 11.9516 (6), 5.4594 (3)	5.1008 (3), 11.9558 (8), 5.4602 (3)
β (°)	111.784 (2)	111.781 (2)	111.772 (3)
V (Å^3)	308.78 (3)	309.00 (3)	309.23 (3)
Z	1	1	1
D_x (Mg m^{-3})	1.615	1.613	1.612
Radiation type	Neutron radiation	Neutron radiation	Neutron radiation
Wavelength (Å)	0.8395	0.8395	0.8395
No. of reflections for cell parameters	1319	1062	1070
θ range (°)	4.03–45.02	4.03–46.20	4.03–39.99
μ (mm^{-1})	0.239	0.239	0.239
Temperature (K)	288 (2)	301 (2)	304 (2)
Crystal form, colour	Needle, clear	Needle, clear	Needle, clear
Crystal size (mm)	6 × 1.8 × 1.7	6 × 1.8 × 1.7	6 × 1.8 × 1.7
Data collection			
Diffractometer	D9	D9	D9
Data collection method	Equatorial geometry scans	Equatorial geometry scans	Equatorial geometry scans
Absorption correction	Gaussian	Gaussian	Gaussian
T_{min}	0.5504	0.5933	0.5934
T_{max}	0.7061	0.7060	0.7060
No. of measured, independent and observed parameters	1540, 1319, 1249	1062, 927, 872	1070, 926, 861
Criterion for observed reflections	$I > 2\sigma(I)$	$I > 2\sigma(I)$	$I > 2\sigma(I)$
R_{int}	0.0159	0.0209	0.0175
θ_{max} (°)	45.02	46.20	39.99
Range of h, k, l	$-8 \rightarrow h \rightarrow 2$ $-13 \rightarrow k \rightarrow 18$ $-6 \rightarrow l \rightarrow 9$	$-7 \rightarrow h \rightarrow 2$ $-13 \rightarrow k \rightarrow 18$ $-7 \rightarrow l \rightarrow 8$	$-7 \rightarrow h \rightarrow 2$ $-13 \rightarrow k \rightarrow 18$ $-6 \rightarrow l \rightarrow 8$
No. and frequency of standard reflections	3 every 50 reflections	3 every 50 reflections	3 every 50 reflections
Intensity decay (%)	0	0	0
Refinement			
Refinement on	F^2	F^2	F^2
$R[F^2>2\sigma(F^2)]$, $wR(F^2)$, S	0.0371, 0.0777, 1.204	0.0267, 0.0614, 1.154	0.0273, 0.0673, 1.087
No. of reflections and parameters used in refinement	1319, 92	927, 92	926, 92
H-atom treatment	Mixture of constrained and independent	Mixture of constrained and independent	Mixture of constrained and independent
Weighting scheme	$w = 1/[\sigma^2(F_o^2) + (0.0324P)^2 + 0.5346P]$ where $P = (F_o^2 + 2F_c^2)/3$	$w = 1/[\sigma^2(F_o^2) + (0.0316P)^2 + 0.3176P]$ where $P = (F_o^2 + 2F_c^2)/3$	$w = 1/[\sigma^2(F_o^2) + (0.0408P)^2 + 0.3169P]$ where $P = (F_o^2 + 2F_c^2)/3$
$(\Delta/\sigma)_{max}$	<0.001	<0.001	<0.001
$\Delta\rho_{max}$, $\Delta\rho_{min}$ (f Å^{-3})	0.681, −0.622	0.47, −0.441	0.47, −0.596
Extinction method	*SHELXL*	*SHELXL*	*SHELXL*
Extinction coefficient	0.615 (18)	0.583 (17)	0.568 (18)

	313 K	323 K	427 K
Crystal data			
Chemical formula	$C_8H_{20}N_4O_8$	$C_8H_{20}N_4O_8$	$C_8H_{20}N_4O_8$
Chemical formula weight	300.24	300.24	300.24
Cell setting, space group	Monoclinic, $P2_1/n$	Monoclinic, $P2_1/n$	Monoclinic, $P2_1/n$
a, b, c (Å)	5.1012 (3), 11.9651 (9), 5.4604 (4)	5.1026 (3), 11.9752 (9), 5.4602 (4)	5.1074 (3), 12.0775 (9), 5.4596 (4)
β (°)	111.763 (5)	111.757 (5)	111.827 (5)
V (Å^3)	309.53 (4)	309.88 (4)	312.63 (4)
Z	1	1	1
D_x (Mg m^{-3})	1.611	1.609	1.595
Radiation type	Neutron radiation	Neutron radiation	Neutron radiation
Wavelength (Å)	0.8395	0.8395	0.8397
No. of reflections for cell parameters	1044	926	399
θ range (°)	4.02–39.96	4.02–39.93	3.99–46.23
μ (mm^{-1})	0.239	0.239	0.239
Temperature (K)	313 (2)	323 (2)	427 (2)
Crystal form, colour	Needle, clear	Needle, clear	Needle, clear

Table 1 (continued)

	313 K	323 K	427 K
Crystal size (mm)	6 × 1.8 × 1.7	6 × 1.8 × 1.7	6 × 1.8 × 1.7
Data collection			
Diffractometer	D9	D9	D9
Data collection method	Equatorial geometry scans	Equatorial geometry scans	Equatorial geometry scans
Absorption correction	Gaussian	Gaussian	Gaussian
T_{min}	0.5934	0.5936	0.5936
T_{max}	0.7060	0.7060	0.7060
No. of measured, independent and observed parameters	1044, 926, 876	1060, 926, 883	399, 331, 312
Criterion for observed reflections	$I > 2\sigma(I)$	$I > 2\sigma(I)$	$I > 2\sigma(I)$
R_{int}	0.0149	0.0214	0.0929
θ_{max} (°)	39.96	39.93	46.23
Range of h, k, l	$-7 \rightarrow h \rightarrow 2$ $-13 \rightarrow k \rightarrow 18$ $-6 \rightarrow l \rightarrow 8$	$-7 \rightarrow h \rightarrow 2$ $-13 \rightarrow k \rightarrow 18$ $-6 \rightarrow l \rightarrow 8$	$-5 \rightarrow h \rightarrow 1$ $-4 \rightarrow k \rightarrow 12$ $-7 \rightarrow l \rightarrow 6$
No. and frequency of standard reflections	3 every 50 reflections	3 every 50 reflections	3 every 50 reflections
Intensity decay (%)	0	0	0
Refinement			
Refinement on	F^2	F^2	F^2
$R[F^2>2\sigma(F^2)]$, $wR(F^2)$, S	0.03, 0.0741, 1.159	0.0311, 0.0746, 1.155	0.0314, 0.0718, 1.333
No. of reflections and parameters used in refinement	926, 92	926, 92	331, 92
H-atom treatment	Mixture of constrained and independent	Mixture of constrained and independent	Mixture of constrained and independent
Weighting scheme	$w = 1/[\sigma^2(F_o^2) + (0.0434P)^2 + 0.2935P]$ where $P = (F_o^2 + 2F_c^2)/3$	$w = 1/[\sigma^2(F_o^2) + (0.0434P)^2 + 0.2935P]$ where $P = (F_o^2 + 2F_c^2)/3$	$w = 1/[\sigma^2(F_o^2) + (0.0434P)^2 + 0.2935P]$ where $P = (F_o^2 + 2F_c^2)/3$
$(\Delta/\sigma)_{max}$	<0.001	<0.001	0.001
$\Delta\rho_{max}$, $\Delta\rho_{min}$ (f Å^{-3})	0.508, −0.551	0.614, −0.645	0.605, −0.353
Extinction method	*SHELXL*	*SHELXL*	*SHELXL*
Extinction coefficient	0.60 (2)	0.59 (2)	0.26 (2)

Computer programs used: ILL *MAD*, ILL *RAFD9*, ILL *RETREAT*, *SHELXL*97 (Sheldrick, 1997).

consists of layers of molecules perpendicular to the crystallographic *b*-axis direction and linked by short N(3)—H(6)···O(1) and N(3)—H(7)···O(2) hydrogen bonds. These layers contain image and mirror-image entities. Two single layers are held together by a longer N(3)—H(8) hydrogen bond bifurcated between O(1) of one molecule and O(2) of another, both in the neighbouring layer, to form antiparallel double layers. Each molecule in one plane of this double layer is therefore hydrogen bonded to four molecules in the adjacent plane. Between different double layers, no N—H···O hydrogen bonding occurs, although there are weak C—H···O interactions (Fig. 1).

Recent electrical impedance measurements of single-crystal α-glycine have revealed anomalous temperature dependence of the conductance and capacitance above ambient temperature (Chilcott *et al.*, 1999). Upon cooling the crystal from 323 K, the conductance decreases slowly from an initial value of 0.1 nS to about 0.02 nS at 304 K. Further cooling, however, causes a dramatic increase in conductance, with a magnitude approaching 100 nS at 294 K. Similar anomalous behaviour is exhibited by the capacitance; it is approximately temperature independent above 304 K, decreases below this temperature to a negative value at 294 K, but upon further temperature decrease becomes positive and quite large.

The usual mechanisms used to explain insulating single crystals cannot provide an explanation for these observations. Rather, it has been proposed (Chilcott *et al.*, 1999) that pyroelectricity occurs as a result of a phase transition of the α-glycine crystals, perhaps similar to the order–disorder ferroelectric transitions in the extensively studied crystals of triglycine sulfate (Xu, 1991) and glycine phosphite (Tritt-Goc *et al.*, 1998). Pyroelectricity can only arise in non-symmetric materials. At equilibrium, any heat applied to a crystal will be isotropic, and for a crystal to develop charges of opposite sign at opposite ends of a line through its macroscopic centre, it must not have a centre of symmetry. The onset of pyroelectricity must therefore be accompanied by a change from the centrosymmetric space group $P2_1/n$ to a non-centrosymmetric

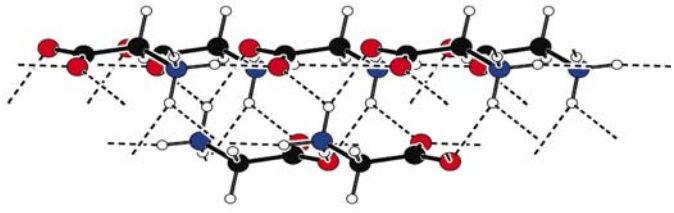

Figure 1
A view perpendicular to the *b*-axis direction of α-glycine showing a hydrogen-bonded antiparallel double layer. Oxygen, carbon, nitrogen and hydrogen atoms are represented by red, black, blue and white spheres, respectively. The bifurcated hydrogen bonds between single layers are represented by dashed lines.

space group, or the breakdown of centrosymmetry as a result of disorder.

Although X-ray and neutron diffraction studies of α-glycine have been reported at around room temperature (~298 K) there has been no attempt to investigate structural changes above room temperature. In this study we have therefore used neutron diffraction in order to characterize the crystal structure of α-glycine over the temperature interval associated with anomalous electrical properties. We have used neutrons for two reasons. Firstly, changes in hydrogen bonds might by expected to be crucial to the phenomena discussed above and only high-resolution neutron diffraction can give precise information about the expected subtle changes in hydrogen-atom positions. Secondly, exposure of α-glycine crystals to X-rays is known to produce free radicals (Sanderud & Sagstuen, 1998) and X-ray-generated free radicals are known to shift T_c in glycine-containing ferroelectric crystals (Strukov *et al.*, 1997).

2. Experimental

Large single crystals were grown by allowing a supersaturated aqueous solution to cool from 353 K to ambient at a rate of about 1 K every 30 min. Measurements were carried out on D9, a four-circle diffractometer optimized for very precise measurements, at the high-flux reactor run by the Institut Laue Langevin. Data sets were collected at 288, 301, 304, 313 and 323 K. A further data set with slightly lower resolution was measured at 427 K from the same crystal at a later date in order to investigate whether the observed temperature-dependent trends extended beyond the initial temperature range. Data, including systematically absent reflections, were collected in resolution shells, $0 < 2\theta < 50^\circ$, $50 < 2\theta < 70^\circ$ and $2\theta > 70^\circ$. The data were complete to $2\theta < 70^\circ$, but incomplete in the higher resolution shell owing to a lack of time. In general, more accurate cell parameters can be deduced by X-ray diffraction. However, because of the possible introduction of free-radical effects, we decided to rely on the unit-cell parameters deduced from the neutron data, using all reflections. The details of the data collections and refinements at all six temperatures are given in Table 1. Full details of all refinements have been deposited as supplementary material.[1]

3. Results

Careful inspection of the space-group absences showed no indication of a space group change with temperature. Neither was there any indication of twinning or a large increase in disorder. However, the unit cell expands in a very anisotropic manner. Fig. 2 shows the unit-cell parameters reported in this study along with those determined previously at 15 K (Peeters *et al.*, 1995) and 120 K (Almof *et al.*, 1973) as a function of temperature. The most striking feature of this plot is the large increase in b with increasing temperature. The relative change in b is far greater than the changes in the other lattice parameters and over the temperature interval of interest becomes directly proportional to the change in unit-cell volume.

The geometrical parameters of the molecule and its orientation in the unit cell do not change significantly with temperature. The short invariant intermolecular intraplanar hydrogen-bond N(3)—H(6)···O(1) lies directly along the c-axis direction and may partly explain the invariance of the unit cell in this direction. The only significant structural change is in the minor component of the bifurcated hydrogen bond that links molecular layers stacked in the b-axis direction. The donor–acceptor ($D\cdots A$) distance of the minor component of the interplanar hydrogen bond increases by 0.015 (1) Å from 3.065 (1) Å at 288 K to 3.080 (1) Å at 323 K. There is a corresponding increase of 0.014 (4) Å from 2.101 (2) Å at 288 K to 2.115 (3) Å at 323 K in the H···A distance. The $D\cdots A$ distance increases further by 0.050 (3) Å

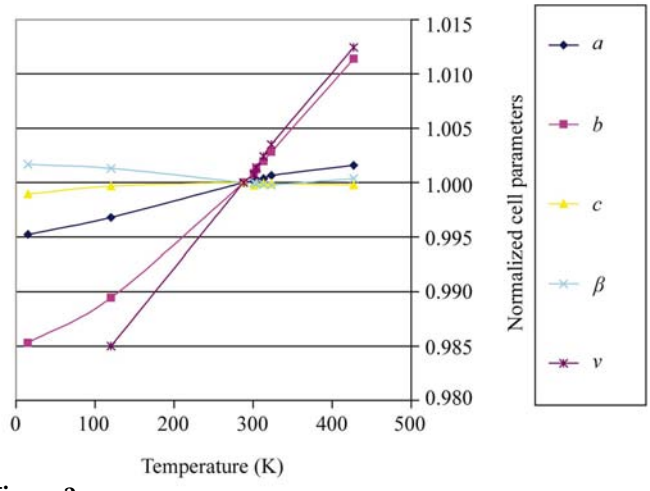

Figure 2
Temperature variation of α-glycine unit-cell parameters normalized with respect to those at 288 K. Values previously determined at 15 K (Peeters *et al.*, 1995) and 120 K (Almof *et al.*, 1973) are also shown. Previously reported room-temperature values have not been included because of the uncertainty in the exact temperature.

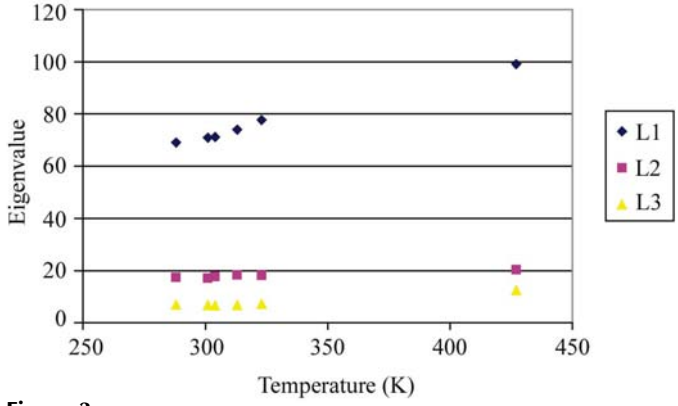

Figure 3
Temperature variation of the eigenvalues of the libration tensor for α-glycine.

[1] Supplementary data for this paper are available from the IUCr electronic archives (Reference: AN0604). Services for accessing these data are described at the back of the journal.

to 3.130 (3) Å at 427 K with a corresponding increase by 0.100 (8) Å to 2.215 (7) Å in the H···*A* distance. However, the short H···*A* distance reported at 120 K [2.049 (1) Å] indicates that this change in hydrogen-bond strength is associated with thermal expansion and is not more pronounced in the temperature range of interest here.

In order to test if libration could be responsible for the anisotropic expansion along the *b*-axis direction, a rigid-body analysis was carried out at each temperature. The program *PLATON* (Spek, 1990) was used to calculate the Schomaker–Trueblood **TLS** tensors (Schomaker & Trueblood, 1968), where the **T**, **L** and **S** represent translation motion, libration motion and the correlation between the two. The definition of the rigid body included hydrogen atoms, because of the small size of the molecule and the need to avoid a singularity. The **S** matrix was small enough to be neglected at all temperatures. The libration motion in particular is very anisotropic with the largest r.m.s. amplitude of libration, *L*1, at all temperatures lying along an axis that is approximately parallel to the molecular bonds C(4)—C(5), N(3)—H(6), and to the unit cell *c*-axis direction (Fig. 3). Librations around this axis will result in the displacement of atoms out of the molecular plane and along the *b*-axis direction.

The translation motion of the centre of mass of the rigid body also changes with temperature (Fig. 4). Eigenvalues *T*1 and *T*2 correspond to translation motions along axes that lie approximately in the molecular planes and perpendicular to the crystallographic *b*-axis direction. These motions increase in an approximately linear fashion with temperature. A smaller translation motion, represented by *T*3, takes place along the *b*-axis direction. There is an apparent anomaly in *T*3 at 427 K that will require further investigation. Although the translation motions show a larger percentage increase with temperature than the libration motions, they represent smaller relative displacements for most atoms. The variation in the rate of increase in U_{22} with temperature for all non-H atoms systematically decreases across the molecule from the terminal O(1), O(2) atoms and the N(3) atoms to the central C(4) and C(5) atoms (Fig. 5). This confirms that the molecule is moving as a rigid body and that the major component is a libration affecting atom displacements in the *b*-axis direction, with the carbonyl C(4) atom close to a pivot point. The linear dependence of *L*1 on temperature suggests that the molecule librates approximately as a simple harmonic oscillator. The resulting temperature dependent motion of atoms in the *b*-axis direction caused by libration can be correlated with the anisotropic expansion of the unit cell in this direction. Rigid-body model libration corrections for bond distances were calculated but these corrections did not increase significantly with temperature (Schomaker & Trueblood, 1968).

4. Discussion and conclusions

The results of this study indicate that the changes in space-group symmetry or disorder required for the onset of pyroelectricity do not occur. Pyroelectricity therefore cannot explain the anomalous electronic properties in this temperature range. There is, however, a very anisotropic expansion in the unit-cell parameters with temperature that has the effect of separating the molecular layers with increasing temperature and lengthening the minor component of the interlayer bifurcated hydrogen bond. This layer separation can be correlated with a large and anisotropic libration motion.

A change in polarization as a result of the change in interlayer hydrogen-bond strength with temperature cannot explain the anomalous electronic properties. The change in H···*A* length corresponds to a change in bond strength of only a few percent (~400 J mol^{-1}) which will not greatly affect the dipole moment associated with the *D*—H group. However, because each oxygen atom of the carbonyl group accepts more than one hydrogen bond, it might be expected that a change in the balance of strength of these hydrogen bonds would change the polarization of this group. The delocalized part of the electron distribution is most likely to be affected by such a change, because its large distance from the oxygen nuclei implies large polarizability. However, there is no significant change in the relative lengths of the C(4)—O(1) and C(4)—

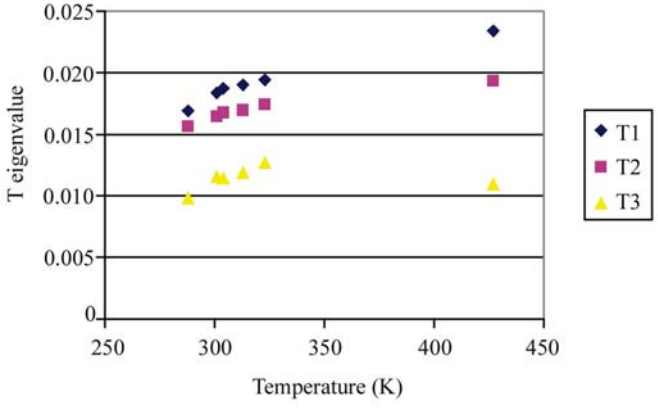

Figure 4
Temperature variation of the eigenvalues of the translation tensor for α-glycine.

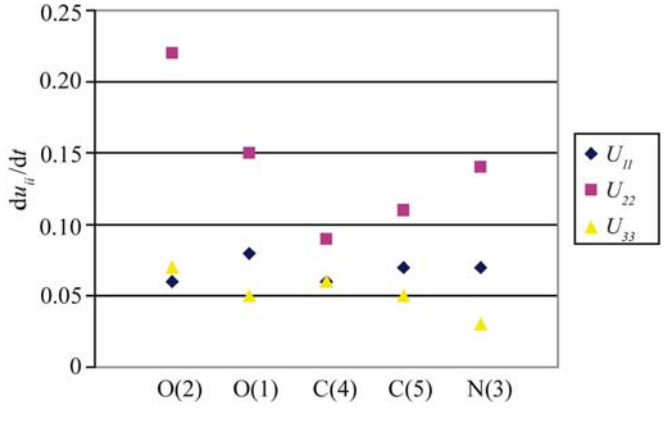

Figure 5
The variation in the rate of increase in each u_{ii} value with temperature (du_{ii}/dT) across all non-H atoms for α-glycine [from left to right: O(2), O(1), C(4), C(5), N(3)].

O(2) bonds or the O(1)—C(4)—O(2) angle which could suggest a change in the distribution of the delocalized electron density.

The glycine molecule itself possesses a relatively large dipole moment (a few 10^{-29} Cm) lying approximately along the molecular axis because of its zwitterionic form. Molecular dipoles within each molecular plane lie in the same direction, corresponding approximately to the crystallographic *c* axis. Molecular dipole moment directions in adjacent planes are antiparallel and the crystal can be thought of as antiferroelectric. There is no evidence in this study of any type of ferroelectric spontaneous polarization in the absence of an applied electric field, resulting from reorientation of individual molecular dipoles within these planes as a function of temperature.

The reported low signal frequency used in measuring the anomalous electronic effects (0.8 Hz) is much smaller than any molecular rigid-body motion, so it follows that the molecular dipoles can be aligned in an applied field. The contribution of the alignment of molecular dipoles to the total polarizability of the crystal will be much greater than contributions from electronic or ionic polarizabilities. From the results of this study we conclude that the main features of the reported anomalous electronic properties of α-glycine most likely arise from libration-driven changes in the interaction and separation of molecular layers that alter the ability of molecular dipoles to reorient in response to an applied electric field. It is well known that changes in stacking interactions between antiferroelectric molecular dipole layers can have large effects on the dielectric properties of liquid crystals in the absence of applied electric fields. It is also well known that changes in temperature can greatly influence the possibility of field-induced antiferroelectric to ferroelectric transitions in a wide variety of materials.

It should be noted that in addition to individual molecular dipole reorientations, collective reorientation could be important in determining electrical properties. Paradoxically, although the weakening of the minor component of the bifurcated bond with increasing temperature would appear to be driven by an increase in librational motion, the other hydrogen bonds do not seem to be affected by this motion. One possible explanation for the preservation of these hydrogen bonds is the existence of collective motions in which aggregates, possibly sheets of molecules, exhibit correlated motions. A second-order phase transition to a high-temperature plastic phase of aggregates of hydrogen-bonded molecules has recently been put forward as an explanation for a slow increase in conductivity with temperature in crystals of *m*-nitroaniline in the temperature region just above ambient (Wójcik & Holband, 2001).

We thank Chris Ling for the neutron diffraction results at 427 K, Jacqui Cole and Garry McIntyre for helpful discussions, the Institut Laue Langevin for the provision of facilities, and the US Department of Energy for financial support.

References

Albrecht, G. & Corey, R. B. (1939). *J. Am. Chem. Soc.* **61**, 1087–1093.
Almof, J., Kvick, A. & Thomas, J. O. (1973) *J. Chem. Phys.* **59**, 3901–3906.
Chilcott, T. C., Schoenborn, B. P., Cooke, D. W. & Coster, H. G. L. (1999). *Phil. Mag. B*, **79**, 1695–1701.
Iitaka, Y. (1960). *Acta Cryst.* **13**, 35–45.
Iitaka, Y. (1961). *Acta Cryst.* **14**, 1–10.
Jonsson, P. & Kvick, A. (1972). *Acta Cryst.* **B28**, 1827–1833.
Kvick, A., Canning, W. M., Koetzle, T. F. & Williams, G. J. B. (1980). *Acta Cryst.* B**36**, 115–120.
Legros, J. P. & Kvick, A. (1980). *Acta Cryst.* B**36**, 3052–3059.
Nyberg, M., Hasselstrom, J., Karis, O., Wassdahl, N., Weinelt, M., Nilsson, A. & Pettersson, L. G. M. (2000). *J. Chem. Phys.* **112**, 5420–5427.
Peeters, A., Alsenoy, C. V., Lenstra, A. T. H. & Geise, H. J. (1995). *J. Chem. Phys.* **103**, 6608–6616.
Power, L. F., Turner, K. E. & Moore, F. H. (1976). *Acta Cryst.* B**32**, 11–16.
Sanderud, A. & Sagstuen, E. (1998). *J. Phys. Chem. B*, **102**, 9353–9361.
Schomaker, V. & Trueblood, K. N. (1968). *Acta Cryst.* B**24**, 63–76.
Sheldrick, G. M. (1997). *SHELXL*. University of Göttingen, Germany.
Spek, A. L. (1990). *Acta Cryst.* A**46**, C-34
Strukov, B. A., Taraskin, S. A. & Song, Y. W. (1997). *Ferroelectrics*, **192**, 293–302.
Tritt-Goc, J., Pislewski, N., Szczepanska, L. & Goc, R. (1998). *Solid State Commun.* **108**, 189–192.
Wójcik, G. & Holband, J. (2001). *Acta Cryst.* B**57**, 346–352.
Xu, Y. (1991). *Ferroelectric Materials and their Applications*. Amsterdam: Elsevier.